



Hybrid [¹⁸F]-F-DOPA PET/MRI Interpretation Criteria and Scores for Glioma Follow-up After Radiotherapy

Marc Bertaux¹ · Arnaud Berenbaum¹ · Anna-Luisa Di Stefano² · Laura Rozenblum¹ · Marine Soret^{1,3} · Sebastien Bergeret¹ · Khé Hoang-Xuan² · Laure-Eugenie Tainturier¹ · Brian Sgard¹ · Marie-Odile Habert^{1,3} · Jean-Yves Delattre² · Caroline Dehais² · Ahmed Idbaih² · Nadya Pyatigorskaya^{4,5} · Aurelie Kas^{1,3}

Received: 15 October 2021 / Accepted: 6 January 2022 / Published online: 11 February 2022
© The Author(s), under exclusive licence to Springer-Verlag GmbH Germany 2022

Abstract

Objective ¹⁸F-fluoro-L-3,4-dihydroxyphenylalanine positron emission tomography (F-DOPA PET) is used in glioma follow-up after radiotherapy to discriminate treatment-related changes (TRC) from tumor progression (TP). We compared the performances of a combined PET and MRI analysis with F-DOPA current standard of interpretation.

Methods We included 76 consecutive patients showing at least one gadolinium-enhanced lesion on the T1-w MRI sequence (T1G). Two nuclear medicine physicians blindly analyzed PET/MRI images. In addition to the conventional PET analysis, they looked for F-DOPA uptake(s) outside T1G-enhanced areas (T1G/PET), in the white matter (WM/PET), for T1G-enhanced lesion(s) without sufficiently concordant F-DOPA uptake (T1G+/PET), and F-DOPA uptake(s) away from hemorrhagic changes as shown with a susceptibility weighted imaging sequence (SWI/PET). We measured lesions' F-DOPA uptake ratio using healthy brain background (TBR) and striatum (T/S) as references, and lesions' perfusion with arterial spin labelling cerebral blood flow maps (rCBF). Scores were determined by logistic regression.

Results 53 and 23 patients were diagnosed with TP and TRC, respectively. The accuracies were 74% for T/S, 76% for TBR, and 84% for rCBF, with best cut-off values of 1.3, 3.7 and 1.25, respectively. For hybrid variables, best accuracies were obtained with conventional analysis (82%), T1G+/PET (82%) and SWI/PET (81%). T1G+/PET, SWI/PET and rCBF ≥ 1.25 were selected to construct a 3-point score. It outperformed conventional analysis and rCBF with an AUC of 0.94 and an accuracy of 87%.

Conclusions Our scoring approach combining F-DOPA PET and MRI provided better accuracy than conventional PET analyses for distinguishing TP from TRC in our patients after radiation therapy.

Keywords Positron emission tomography · Radiolabeled amino acid · Glial tumor · Magnetic resonance imaging · Arterial spin labeling

✉ Marc Bertaux
marc.beraux@gmail.com

- ¹ Service de médecine nucléaire, AP-HP, Hôpitaux Universitaires La Pitié Salpêtrière—Charles Foix, 75013 Paris, France
- ² Inserm, CNRS, UMR S 1127, Institut du Cerveau et de la Moelle épinière, ICM, AP-HP, Hôpitaux Universitaires La Pitié Salpêtrière—Charles Foix, Service de Neurologie 2-Mazarin, Sorbonne Université, 75013 Paris, France
- ³ LIB, INSERM U1146, Sorbonne Université, 75013 Paris, France
- ⁴ Service de neuroradiologie, AP-HP, Hôpitaux Universitaires La Pitié Salpêtrière—Charles Foix, 75013 Paris, France
- ⁵ INSERM U 1127, CNRS UMR 7225, Sorbonne Université, UPMC Univ Paris 06, UMRS 1127, CNRS UMR 7225, Institut du Cerveau et de la Moelle épinière-ICM, Paris, France

Abbreviations

ASL	Arterial spin-labelling
DSC	Dynamic susceptibility contrast
F-DOPA	¹⁸ F-fluoro-L-3,4-dihydroxyphenylalanine
FET	¹⁸ F-fluoroethyl-tyrosine
FLAIR	Fluid-attenuated inversion recovery T2 sequence
IDH	Isocitrate dehydrogenase
OS	Overall survival
PET	Positron emission tomography
RCBF	Regional cerebral blood flow
ROC	Receiver operating characteristic
ROI	Region of interest
SUVmax	Maximum standard uptake value

SWI	Susceptibility-weighted imaging MRI sequence
T/S	Tumor-to-striatum ratio
T1G	MRI T1-weighted sequences after gadolinium contrast agent injection
TBR	Tumor-to-background ratio
TP	Tumor progression
TRC	Treatment-related changes

Introduction

Treatment-related changes (TRC), i.e. pseudoprogression and radionecrosis, can occur during the follow-up of patients with a diffuse glioma after radiation therapy. The TRC and tumor progression (TP) may have a similar aspect in MRI T1-weighted sequences after gadolinium contrast agent injection (T1G) as both can lead to an increased blood-brain barrier permeability. The most widely used technique to differentiate them is MRI perfusion-weighted imaging using the dynamic susceptibility contrast (DSC) technique. In patients with high-grade glioma, the calculation of the normalized regional cerebral blood volume ratio with DSC shows an overall good performance in this setting, with sensitivity and specificity ranging from 0.81 to 0.94 and from 0.78 to 0.95, respectively; however, proposed cut-off values are highly variable across studies [1]. Moreover, the hemorrhagic changes that frequently occur in patients with glioma can lead to magnetic susceptibility artefacts and be responsible for false negative results. Arterial spin-labelling (ASL) perfusion sequence is an alternative to DSC. It also showed good performances in differentiating TP from TRC [2] and should be less prone to susceptibility artefacts, as frequently seen in this setting.

¹⁸F-fluoro-L-3,4-dihydroxyphenylalanine (F-DOPA) positron emission tomography (PET) imaging can be used during the follow-up of patients with glioma, when morphological and advanced MRI results remain equivocal [3]. F-DOPA PET sensitivity to diagnose recurrence is good in both high-grade and low-grade gliomas, ranging from 81% to 95%, but its specificity remains suboptimal, ranging from 66% to 85% [4–7]. The conventional F-DOPA PET method of interpretation is based purely on lesion(s) intensity of uptake. Whether by visual analysis or a region of interest (ROI) based method, F-DOPA uptakes are considered suggestive of TP when their intensity is greater than that of contralateral striatum or twice that of the normal cortex, and suggestive of TRC when it is not [8]. Unlike ¹⁸F-fluoroethyl-tyrosine (FET), the diagnostic value of kinetic analysis has not been shown for F-DOPA in this setting. [9–11].

Current European practice guidelines state that amino acid PET images should be fused and interpreted in conjunction with most recent T1G and T2-weighted sequences

[12]; however, the guidelines do not specify how lesion characteristics on MRI may or may not influence PET images interpretation and how to implement it in clinical practice, as data on the subject are scarce [13, 14]. Yet, misleading F-DOPA PET uptake can occur in inflammatory [15], infectious [16], epileptic [17] and hemorrhagic processes [18]. Some of these features can be specified on MRI. For example, the extracortical localization of an uptake excludes its epileptic origin and massive inflammatory changes in the brain are rarely seen without concordant enhancement in T1G sequences. In addition, susceptibility-weighted imaging MRI sequences (SWI) make it possible to delineate brain regions where bleeding has occurred. Thus, it can be assumed that F-DOPA uptakes are more specific for viable tumor tissue when they are located in the white matter, and/or outside enhanced areas in T1G, and/or outside of hemorrhagic areas on SWI sequences. Conversely, we believe that the presence of a T1G enhanced lesion incompletely matched by an F-DOPA PET uptake could be a good indicator of TRC even when it co-exists with abnormal uptakes elsewhere in the brain.

Based on these hypotheses, the purpose of this exploratory work was to create hybrid parameters and scores combining MRI and PET features to use for clinical routine interpretation of F-DOPA PET scans in glioma patients after radiation therapy, which would outperform the current standard interpretation.

Material and Method

Patients

All patients who underwent an F-DOPA PET/MRI in the nuclear medicine department of the Pitié-Salpêtrière Hospital, Paris, France, for post-radiation therapy follow-up of a histologically proven infiltrating glioma between 1 January 2016 and 31 December 2018 were retrospectively included in our study. Patients were excluded from the analysis if they had no enhanced lesion on MRI. For patients who underwent multiple PET/MRI scans, only the first was analyzed.

All gliomas were classified according to the WHO 2016 classification based on the status of isocitrate dehydrogenase (IDH) genes (mutated versus none mutated) and on 1p19q co-deletion (co-deleted or non-co-deleted). Three subgroups were identified: IDH mutated without 1p-19q co-deletion (IDH_{m-non-codel}), IDH mutated and 1p-19q co-deleted (IDH_{m-codel}), and IDH wild-type (IDH_{WT}).

When available, the definitive diagnosis of TRC or TP was based on histology. In all the other cases, it was the result of an expert consensus based on the Response assessment in neuro-oncology group (RANO) criteria and cur-

rent glioma monitoring guidelines. The latter indicates that a new tumor or brain lesion observed on MRI and/or an obvious increase in the size of the tumor or an increase in contrast enhancement, and/or a significant clinical deterioration, provided that these modifications are not attributable to non-tumor causes, correspond to a recurrence/progression [19, 20]. For the diagnosis to be considered as TP, a new progression had to occur within 3 months following PET/MRI for IDH_{WT}, within 6 months for IDH_{m-non-codel}, and within 12 months for IDH_{m-codel} gliomas. In patients for whom a new treatment had been started after F-DOPA PET/MRI, the time limit was extended to 6 months for IDH_{WT} and to 9 months for IDH_{m-non-codel} gliomas.

The use of patient data was approved by the French authority for the protection of privacy and personal data in clinical research (Commission Nationale de l'Informatique et des Libertés, approval No. 2111722). This study was carried out in accordance with the principles of the Declaration of Helsinki.

Image Acquisition and Postprocessing

The images were acquired with a Signa PET/MR camera (General Electric Healthcare®, Milwaukee, WI, USA) combining a 3T MR and a SiPM-PET, using an 8-channel head coil. Patients had to fast for at least 4h before the examination and were not given any premedication. PET images were acquired 10min after the intravenous injection of 2 MBq/kg of F-DOPA for 20min. They were reconstructed with an iterative algorithm (OSEM-3D, 28 subsets, 8 iterations, 4mm transaxial Gaussian postfiltering, matrix 256×256) using time of flight and point spread function modelling. Attenuation correction was done using a 2-point Dixon MR sequence that was segmented into three components and supplemented by the use of a single atlas to capture bone information [21].

For this study, we used native and contrast-enhanced (injection of 0.2ml/kg of Dotarem® 90s before acquisition) sagittal 3D T1 spin-echo sequences (TR=602ms,

TE=16.7ms, voxel size 0.5×0.5×1.2mm), axial 3D SWAN sequence (TR=68.5ms, TE=28.1ms, voxel size 0.39×0.39×3.2mm), and the 3D pseudo-continuous ASL sequence (post-label delay=2025ms, TR=4833ms, TE=10.7ms, bandwidth 976.6Hz/pixel, flip angle=111.1°, voxel size 1.875×1.875×4mm). The ASL sequences were postprocessed with the dedicated software using the advantage windows server version 3.2 solution (General Electric Healthcare®) to obtain cerebral blood flow (rCBF) maps. Fluid-attenuated inversion recovery (FLAIR) T2 sequences that are routinely performed for our neuro-oncological patients were not used in this study.

Blind Image Analysis

Two nuclear medicine physicians reviewed the images using the VB 30 version of the imaging software Syngo.via (Siemens Healthcare®, Munich, Germany). They performed a blind examination where the patients' diagnoses and results, as well as their clinical parameters, previous MRI, and request for examination, were not known.

A conventional PET analysis was performed first, using only PET images. Patients were visually classified as positive or negative depending on whether or not there was an encephalic area with an intense F-DOPA uptake. Intense uptake was visually defined as higher than twice the background cortex intensity. This was performed using the SUV100 manufacturer's color scale, adjusted so that the healthy cortex maximum intensity was in the middle of the color range (dark green). Thus, intense uptake areas appeared in the upper color of the range (pink).

For hybrid PET and MRI combined analysis we defined the notion of valid PET uptake as follows: when situated in any T1G enhanced or cortical areas, an F-DOPA uptake had to be intense to be considered valid. In the non enhanced white matter, any visible F-DOPA uptake was considered valid. Then, we defined four binary morphometabolic parameters to be visually classified by reviewers (Table 1). After T1 and T1G sequences were fused with PET images,

Table 1 Summary of visual semi-quantitative parameters

Definitions	Intense F-DOPA uptake: more than twice the healthy brain uptake		Valid F-DOPA uptake: intense in T1G-enhanced or cortical areas, any visible uptake in the non-enhanced white matter		
Parameter	Conventional PET analysis (+ or -)	T1G+/PET (+ or -)	T1G-/PET (+ or -)	WM/PET (+ or -)	SWI/PET (+ or -)
Set(s) of data used	PET	T1G and PET	T1G and PET	T1G and PET	SWI and PET
Criteria for positivity	Any intense uptake	Every T1G enhanced lesion >2cm is matched with intense uptake in more than 60% of their volume	Any valid uptake outside T1G enhanced lesion	Any valid uptake in the white matter	Any valid uptake outside blood products deposition induced SWI hypointensities

T1G T1 weighted sequences after gadolinium contrast agent injection, SWI susceptibility-weighted imaging MRI sequence, "+ or -" means that each of those binary criteria can be either positive or negative in a given patient, F-DOPA ¹⁸F-fluoro-L-3,4-dihydroxyphenylalanine

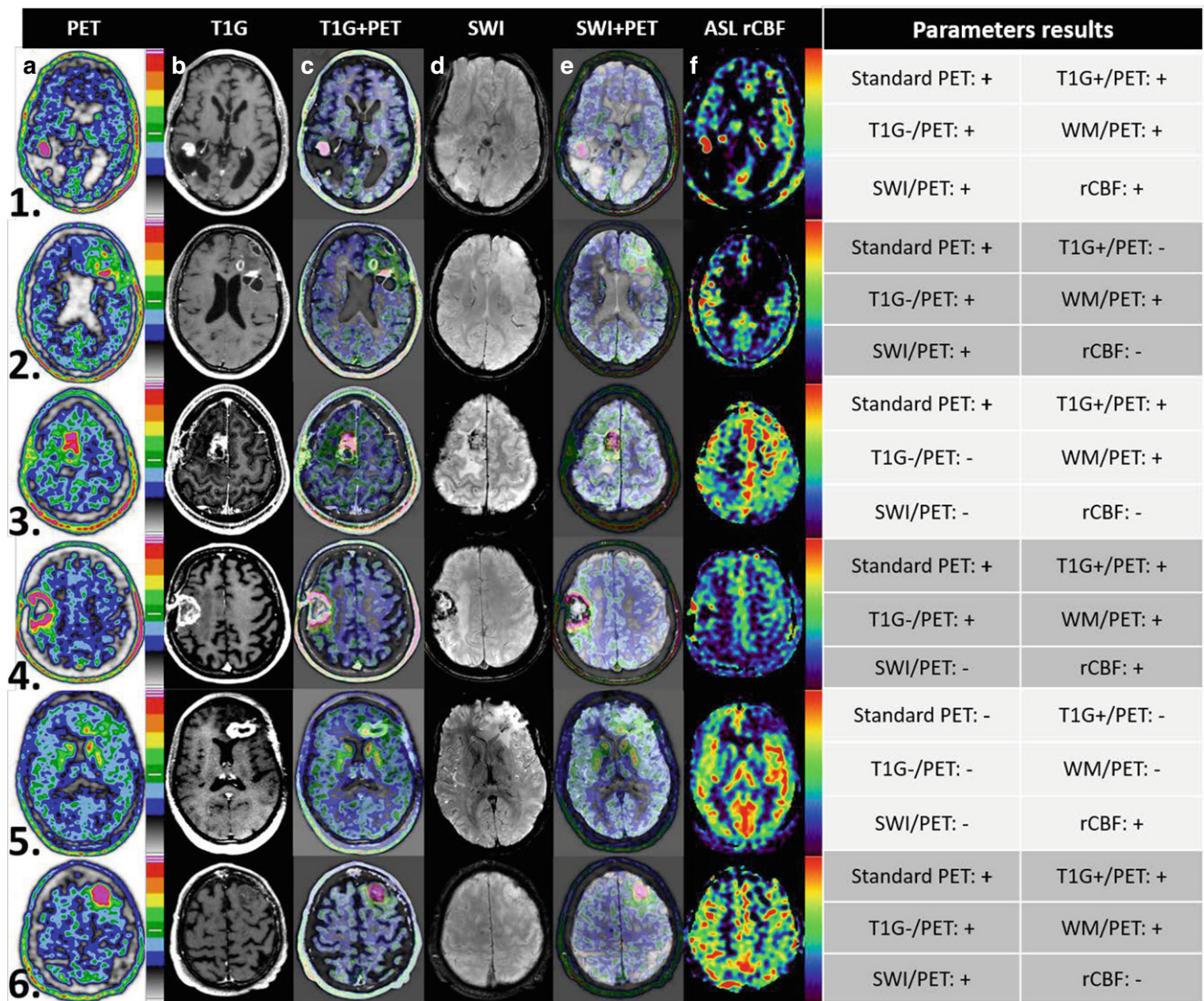


Fig. 1 Examples of PET and MRI hybrid analysis in 6 patients. **a** Conventional visual F-DOPA PET analysis with SUV100 color scale. It is set so that the normal cortex maximum uptake is in the middle of the scale (dark green). The areas with intense F-DOPA uptake (at least twice the normal cortex uptake) are thus represented by the highest intensity color (pink). Conventional analysis is considered positive if any intense uptake is visible. **b** T1G. **c** Fusion between **a** and **b**. T1G+/PET is classified as negative if any contrast-enhanced lesion has more than 40% of its volume without F-DOPA intense uptake. T1G-/PET and WM/PET are classified as positive if any valid F-DOPA uptake is seen outside contrast-enhanced lesion(s) or in the white matter, respectively. When localized in T1G-enhanced areas or the grey matter, an F-DOPA uptake is considered valid only when intense. In the non-enhanced white matter, it is considered valid whenever visible. **d** SWI sequence. Areas where hemorrhagic changes occurred appear hypointense. **e** Fusion between **c** and **d**. SWI/PET is classified as positive if any valid F-DOPA uptake is seen outside the vicinity of SWI hypointense areas. **f** CBF as calculated with ASL sequence (ASIST color scale). Quantitative analysis of rCBF ratio is used instead of visual analysis. F-DOPA images are used to help position regions of interest. Patient 1: Suspicion of IDH_{WT} glioblastoma recurrence 3 years after chemoradiotherapy. Histological analysis after surgical resection showed glioblastoma recurrence. Patient 2: Suspicion of IDH_{m-non-codel} glioblastoma recurrence 4 months after the end of radio-chemotherapy. Monthly temozolomide was continued for another 4 months. Subsequent MRI showed a decrease in T1G enhancements. The final diagnosis was TRC. Patient 3: Suspicion of IDH_{WT} type glioblastoma recurrence 4 months after the end of radio-chemotherapy. Monthly temozolomide chemotherapy was continued for another 5 months until TP occurred in a different localization than the present lesion. The final diagnosis was TRC. Patient 4: Suspicion of IDH_{WT} glioblastoma progression 8 months after the end of radio-chemotherapy. The final diagnosis was TP. Patient 5: Suspicion of IDH_{WT} glioblastoma progression 2 months after the end of radio-chemotherapy. No valid F-DOPA uptake is seen (conventional analysis (-), T1G-/PET (-), SWI/PET (-), WM/PET (-)), with most of the ring-enhanced lesion showing only faint uptake (T1G+/PET (-)). ASL shows a tiny hyperperfused area in the most medial and posterior part of the ring-enhanced lesion, which is easily recognized because it corresponds to the F-DOPA hottest spot. The patient was finally classified as TP and died one year later despite multiple treatment changes. Patient 6: Suspicion of oligodendroglioma recurrence more than 10 years after surgery and radiation therapy. An intense PET uptake entirely covers the focally slightly enhanced left frontal lobe lesion without corresponding SWI hypointense area (conventional analysis (+), T1G-/PET (+), T1G+/PET (+), SWI/PET (+)). No ASL hyperperfusion is found. The final diagnosis was TP, as histological analysis after surgical resection showed grade II oligodendroglioma IDH m-codel tumor recurrence. T1G MRI T1 weighted sequence after gadolinium contrast agent injection, SWI susceptibility-weighted imaging MRI sequence, CBF Cerebral blood flow, ASL arterial spin labelling, F-DOPA ¹⁸F-fluoro-L-3,4-dihydroxyphenylalanine, IDH Isocitrate dehydrogenase

the first parameter, T1G+/PET, was defined as positive if each gadolinium-enhanced lesion of at least 20mm was matched with a PET intense uptake in more than 60% of its volume (T1G+/PET (+)). As such, this parameter was negative if any enhanced lesion of this size was not matched with this type of PET uptake (T1G+/PET (-)). Lesions of less than 20mm were not considered here as PET poor spatial resolution may impact quantification and visual semi-quantification too much in such small objects. The second parameter, T1G-/PET, was classified as positive when any valid F-DOPA uptake was found outside MRI enhanced areas (T1G-/PET (+)), and as negative when none was found outside MRI enhanced areas (T1G-/PET (-)). The third parameter, WM/PET, was classified as positive when any valid F-DOPA uptake could be seen in the white matter (WM/PET (+)), and as negative when none could be found in the white matter (WM/PET (-)). Then, a fusion between PET images and SWI sequence was performed to define the fourth parameter, SWI/PET, and reviewers searched for the presence (SWI/PET (+)) or absence (SWI/PET (-)) of any valid PET uptake outside of susceptibility artefact-induced hypointensities, i.e. not related to hemorrhagic changes. Fig. 1 examples illustrate these morphometabolic parameters.

Quantitative Analysis

For PET, we measured the maximum standard uptake value (SUV_{max}) of the most intense lesion in each patient. The ratios to the contralateral striatal SUV_{max} (T/S) and the healthy brain SUV_{mean} (TBR) were then calculated. The latter was measured using a spherical peripheral 3cm³ volume of interest drawn in the periphery of the contralateral parietal lobe.

For MRI, the size of the enhanced lesion was measured by the product of axial perpendicular short and long axes of the greatest enhanced lesion. A lesion rCBF mean value was obtained for each patient, using a 0.6cm² circular ROI located on the abnormal area showing the highest perfusion. PET images were used to distinguish relevant hot spots from physiological cortex perfusion and vessels. When there was no obvious abnormal perfusion hot spot, the ROI was positioned on the most intense PET uptake. The normalization of these rCBF values to the contralateral semi-oval white matter rCBF mean value was performed to obtain rCBF ratios, except for purely cortical lesions, in which case the normalization was based on cortical contralateral mirrored ROIs.

Statistical Analysis

Kappa interrater reliability coefficients were calculated for morphometabolic binary variables and PET analysis alone.

In the event of divergent results between the two reviewers, a consensus was reached after a joint blind examination of the images which was used for the statistical analyses.

A binary logistic regression using bootstrap analysis (1000 samples) and the enter method was then performed, based on morphometabolic variables, TBR and rCBF ratio as predictors, and diagnosis as the target. A second regression analysis was carried out, using only the parameters that remained statistically significant predictors in the first analysis. The third regression was conducted without rCBF. Multicollinearity between predictive variables was assessed by calculating variance inflation factors. The regression coefficient values finally obtained were used to create morphometabolic scores by rounding off their relative value to the nearest whole number.

Variables are presented as mean ± standard deviation unless otherwise specified. Subgroups variable values were compared using a nonparametric Mann-Whitney. The performances of scores as well as those of rCBF ratio and PET quantitative parameters were compared with receiver operating characteristic (ROC) curve analysis. The best cut-offs were chosen to maximize Youden's index [22]. Accuracies of binary variables were compared with the McNemar test for paired samples and with the χ^2 -test for independent samples.

The patient overall survival (OS) rate was calculated from the date of PET/MRI to the date of death. Kaplan-Meier survival curves were compared with the log-Rank method. A multivariate analysis using the strongest prognostic factors was carried out with the Cox survival model after quantitative variables were dichotomized. To this purpose, optimal cut-offs were identified using X-Tile software (3.6.1, Yale University, New Haven, CT, USA), as well as a follow-up cut-off at 3 years.

All statistical analyses were performed using SPSS 26 software (IBM®, Armonk, NY, USA). A *p*-value of 0.05 or less was considered significant for all the analyses performed.

Results

Patients

In this study 86 consecutive patients referred between January 2016 and December 2018 for an F-DOPA PET/MRI examination were initially included and 5 patients were excluded from the study because of the absence of any enhanced lesion in T1G. Five additional patients, for whom a new treatment line had been started after PET/MRI and who had no tumor progression within the given time frame, were also excluded as a retrospective diagnosis of TP or TRC could not be asserted. Consequently, 76 patients were

included in our analysis (Figure S1 in supplementary materials), of which 23 (30%) were finally diagnosed with TRC and 53 (70%) with TP. The final diagnosis was based on histology in 15 cases (20%) and clinical radiological follow-up in 61 cases (80%).

Gliomas were classified as IDH_{WT} for 36 patients (42%), as IDH_{m-non-codel} for 20 patients (26%) and as IDH_{m-codel} for 18 patients (24%). The molecular profile was not known for 6 patients (8%). Of the patients 17 (22%) underwent PET/MRI within 6 months after radiotherapy, and 59 (78%) after these 6 months. The proportion of TRC (29% and 35%, respectively) was not significantly different between these two subgroups. Also, 31 patients (41%) received chemotherapy in the 6 months before the PET/MRI scan. For them, there was a trend towards a higher proportion of TRC than in other patients, but it did not reach statistical significance (42% versus 22%, $p=0.07$). No significant differences were found in the performances of the diagnostic parameters within these subgroups. Patient characteristics are presented in Table 2.

Table 2 Patient characteristics

Variable	Grouping	N
Sex	Male	40 (53%)
	Female	36 (47%)
Age	Mean (range) in years	53.5 (24–82)
Tumor grade	II	10 (13%)
	III	26 (34%)
	IV	40 (53%)
Neurosurgical management	Maximum safe resection	53 (70%)
	Biopsy only	23 (30%)
Glioma molecular profile	IDH _{m-non-codel}	20 (26%)
	IDH _{m-codel}	18 (24%)
	IDH _{WT}	36 (42%)
	Unknown	6 (8%)
Delay between end of radiotherapy and PET	Median (range) in months	19.2 (1–412)
	6 months or less	17 (22%)
	More than 6 months	59 (78%)
Chemotherapy within 6 months before PET	Temozolomide	27 (36%)
	PCV or lomustine alone	4 (5%)
	None	45 (59%)
Final diagnosis	True progression	53 (70%)
	Treatment-related changes	23 (30%)
Type of proof for final diagnosis	Histology	15 (20%)
	Follow-up	61 (80%)
New line of treatment after PET/MRI	YES	41 (54%)
	NO	35 (46%)

IDH isocitrate dehydrogenase, IDH_{m-non-codel} IDH mutation without 1p19q co-deletion, IDH_{m-codel} IDH mutation and 1p19q co-deletion, IDH_{WT} IDH wild-type glioma, PCV combination of procarbazine, lomustine and vincristine, PET Positron emission tomography

Conventional PET Analysis and Hybrid Parameters Performances

The accuracies to distinguish between TP and TRC were 82% for conventional analysis, 82% for T1G+/PET, 64% for T1G-/PET, 68% for WM/PET, and 80% for SWI/PET. Kappa measurements of interrater reliability were 0.81 for conventional analysis, 0.87 for T1G+/PET, 0.66 for T1G-/PET, 0.77 for WM/PET, and 0.66 for SWI/PET. Qualitative parameters are summarized in Table 3.

Quantitative Parameters Results

Mean T/S (1.6 ± 0.3 vs. 1 ± 0.3), TBR (4.5 ± 1.4 vs. 2.9 ± 1) and rCBF ratio (2.6 ± 1.5 vs. 1.2 ± 0.4) were higher in patients with TP than in those with TRC ($p < 0.001$). The best cut-offs of 1.35 for T/S, 3.7 for TBR and 1.25 for rCBF ratio led to accuracies to differentiate TP from TRC of 74%, 76% and 84%, respectively. These were not significantly different from each other ($p = 0.134$ in between T/S and rCBF). Quantitative parameters are summarized in Table 4.

Scores Construction and Performances

The multicollinearity between variables in the logistic regressions was low or moderate with variance inflation factors lower than 3 in all cases (Table S1). In the first regression analysis, only T1G+/PET, SWI/PET and rCBF ratio were shown to contribute significantly to the model ($p = 0.006$, 0.027 and 0.011 respectively). Using only T1G+/PET, SWI/PET, and a dichotomized version of rCBF ratio with a cut-off of 1.25, the second logistic regression model was able to correctly classify patients in 86% of the cases, with similar beta coefficient values for the 3 parameters (2.3, 1.8, and 2.4, respectively). Using only T1G+/PET and SWI/PET, a model without ASL allowed to correctly classify 83% of the patients, with similar beta coefficient values for both parameters (2.3 and 2.5, respectively).

A 3-point score, with 1 point each for T1G+/PET, SWI/PET and $rCBF \geq 1.25$ was built. With an AUC of 0.93 in ROC analysis, it performed better than T/S (AUC 0.81; $p = 0.001$), TBR (AUC 0.82; $p = 0.003$), rCBF (AUC 0.85; $p = 0.016$) and conventional visual analysis (AUC 0.75 $p < 0.001$) to discriminate between TP and TRC (Fig. 2). Patients presenting a 3-point score of 0 or 1 and those with a score of 2 or 3 were correctly classified as TRC and TP, respectively, with an accuracy of 87%.

A 2-point score using only T1G+/PET and SWI/PET (1 point for each) had an AUC of 0.89, which was higher than with conventional analysis ($p = 0.001$), slightly but not significantly higher than TBR ($p = 0.09$), and slightly but not significantly lower than the 3-point score ($p = 0.085$). Patients with a 2-point score of 0 and those with a score of 1

Table 3 Summary of qualitative parameters and scores

Variable	Result	N	Kappa	χ^2	p-value	AUC	Se (%)	Sp (%)	Acc (%)
<i>Conventional analysis</i>	–	17 (23%)	0.81	19.4	<0.001	0.75	92	57	82
	+	59 (77%)							
<i>T1G+/PET</i>	–	23 (30%)	0.87	21.5	<0.001	0.78	87	70	82
	+	53 (70%)							
<i>T1G-/PET</i>	–	36 (47%)	0.66	5.3	0.021	0.66	62	70	64
	+	40 (53%)							
<i>WM/PET</i>	–	31 (41%)	0.77	6.8	0.009	0.67	70	65	68
	+	45 (59%)							
<i>SWI/PET</i>	–	30 (39%)	0.66	23.2	<0.001	0.81	79	83	81
	+	46 (61%)							
<i>3-point score</i>	0	12 (16%)	N/A	42.5	<0.001	0.93	91	78	87
	1	11 (14%)							
	2	18 (24%)							
	3	35 (46%)							
<i>2-point score</i>	0	16 (21%)	N/A	35.5	<0.001	0.89	94	57	83
	1	21 (28%)							
	2	39 (51%)							

Kappa inter-rater reliability coefficients, AUC area under the curve in ROC analysis, Se sensitivity, Sp specificity, Acc accuracy, TP true progression, TRC treatment-related changes, SWI susceptibility-weighted imaging MRI sequence, *Conventional analysis of F-DOPA PET* positive if there is any intense uptake, that is at least twice the intensity of healthy brain uptake, *T1G+/PET* negative if any T1G contrast-enhanced lesion has no corresponding intense uptake in more than 40% of its volume, as assessed visually, *T1G-/PET* positive if there is any valid F-DOPA PET uptake(s) outside of T1G contrast-enhanced lesion, *WM/PET* positive if there is any valid F-DOPA PET uptake(s) in the white matter. When situated in enhanced or cortical areas, an F-DOPA uptake has to be intense to be considered valid, in the non-enhanced white matter, any visible F-DOPA uptake is considered valid, *SWI/PET* positive if there is any valid F-DOPA PET uptake outside hemorrhagic regions as seen with SWI sequence, *3-point score* 1 point each for T1G-/PET, SWI, and rCBF ≥ 1.25 , *2-point score* 1 point each for T1G-/PET and SWI

Table 4 Summary of quantitative parameters

	N	T/S	TBR	rCBF	Enhancement size (mm ²)
<i>Study population</i>	76	1.4 ± 0.6	4.1 ± 1.5	2.1 ± 1.4	561 ± 752
<i>TP</i>	53	1.6 ± 0.3	4.5 ± 1.4	2.6 ± 1.5	507 ± 632
<i>TRC</i>	23	1 ± 0.3	2.9 ± 1.0	1.2 ± 0.4	684 ± 982
<i>Best cut-off</i>	–	1.35	3.7	1.25	N/A
<i>AUC</i>	–	0.81	0.82	0.85	N/A
<i>Accuracy</i>	–	0.74	0.76	0.84	N/A
<i>For patients with TP and known molecular status (N = 49)</i>					
<i>IDH_{m-non-codel}</i>	11	1.3 ± 0.4	3.7 ± 1.2	2.5 ± 1.8	247 ± 205
<i>IDH_{m-codel}</i>	14	1.8 ± 0.6 ^a	5.1 ± 1.4 ^a	2.1 ± 1.2	323 ± 371
<i>IDH_{WT}</i>	24	1.6 ± 0.5 ^a	4.5 ± 1.3	2.8 ± 1.6	751 ± 784 ^a

All the quantitative parameters, except the enhancement size, were significantly higher in TP than in TRC and able to discriminate between TP and TRC with similar accuracies

TP tumor progression, TRC treatment-related changes, AUC area under the curve in ROC analysis, T/S ratio of lesion SUVmax to striatum SUVmax, TBR ratio of lesion SUVmax to the normal parietal cortex, rCBF regional cerebral blood flow ratio (measured with ASL perfusion), *Enhancement size* product of axial perpendicular diameters of the greatest lesion on T1G sequence, *IDH_{m-non-codel}* IDH mutation without 1p19q co-deletion, *IDH_{m-codel}* IDH mutation and 1p19q co-deletion, *IDH_{WT}* IDH wild-type glioma

^aStatistical significance at the $p=0.05$ threshold with at least one subgroup

or 2 were correctly classified as TRC and TP, respectively, with an accuracy of 83%.

The logistic regression-based predicted probabilities distribution varied between both models. These probabilities were comprised between 0.25 and 0.75 for 22% of the patients in the model without ASL, and for only 13% of them

in the model with ASL (Figures S2 and S3 in supplementary materials). In terms of scores, it meant that a 2-point score of 1 was associated with major diagnostic uncertainty, as 57% of these patients had TP and 43% had TRC. A 3-point score of 2 and 3 were associated with somewhat lower but still important diagnostic uncertainty with a correct classifi-

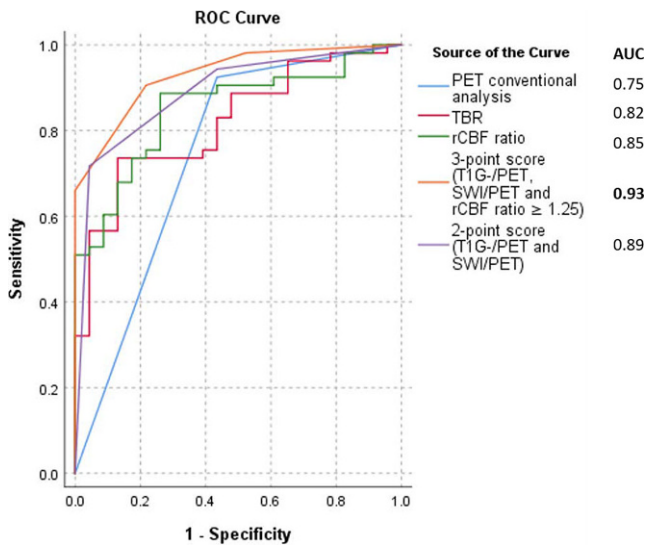


Fig. 2 ROC curves comparison. Receiver operating characteristics curves. TBR ratio of lesion SUVmax to the normal parietal background in F-DOPA PET, PET conventional analysis intensity as based on visual analysis of PET without MRI data, rCBF ratio regional cerebral blood flow ratio (measured with ASL perfusion). The 3-point score is based on logistic regression results using hybrid PET and MRI parameters T1G-/PET, SWI/PET and rCBF ratio with a cut-off at 1.25 (1 point for each). The 2-point score is based on logistic regression performed without ASL rCBF, using T1G-/PET and SWI/PET (1 point for each). The area under the curve (AUC) of the 3-point score (0.931) is significantly higher than for the other parameters, with AUC differences of 0.11 for TBR ($p=0.03$), 0.19 for conventional analysis ($p<0.001$) and 0.08 for ASL ($p=0.02$), with the exception of the 2-point score (AUC difference 0.04 and $p=0.08$)

cation of patients in 64% and 72% of the cases, respectively. On the contrary, a 2-point score of 2 and a 3-point score of 3 were both very strong predictors of TP, with positive predictive values of 97% and 100%, respectively, whereas scores of 0 showed good negative predictive values for TP, of 81% and 92%, respectively.

PET and ASL Features of Different Glioma Subgroups

Among the 53 patients diagnosed with TP, both IDH_{WT} and IDH_{m-codel} gliomas showed higher T/S than IDH_{m-non-codel} tumors ($p=0.008$ and 0.018), while only IDH_{m-codel} lesions had significantly higher TBR than IDH_{m-non-codel} tumors ($p=0.036$ and 0.076). No statistically significant difference was found between tumor groups for rCBF ratio. IDH_{WT} gliomas were associated with enhanced lesions of greater size than other tumors ($p=0.01$ and 0.03). These results are shown in Table 4.

Survival Analyses

The median and mean OS in the whole cohort were 22 and 30 months, respectively. The OS was longer in patients with

TRC than in patients with TP (median not reached versus 18 months, respectively; $p<0.001$; Fig. 3).

Using the Cox model, the tumor molecular profile as well as most PET, MRI and hybrid variables were associated with OS in univariate analysis, with the notable exception of T1G+/PET ($p=0.15$) and T1G/PET ($p=0.55$). In multivariate analyses using best predictors of survival, only molecular profile ($p=0.02$ –0.03) and rCBF ≥ 2.7 ($p=0.03$) were found to be independently and significantly associated with OS. These results are shown in Table 5. The proportional hazards assumption hypothesis was met in all cases.

Discussion

In our study we found that conventional F-DOPA PET analysis based solely on lesion uptake intensity had moderate performances in discriminating between TP and TRC, whether it was measured with volumes of interest or assessed visually in a semi-quantitative manner. In this respect, our results are similar to those of Herrmann et al. [8], who published the largest study on the subject. Indeed, both quantitative analysis (accuracy of 76% for T/S in our study versus 78% for Herrmann et al., for example) and visual semi-quantitative PET analysis (accuracy of 82% but with limited specificity in both studies) had similar performances. We used point spread correction in our study, which probably explains why we found slightly higher best cut-off values than them (T/S = 1.35 vs 1.1 for example).

Some of the morphometabolic semi-quantitative visual parameters we designed were able to discriminate between TP and TRC with fairly good accuracy. Especially, T1G+/PET had an accuracy of 82% and seemed reliable (interobserver Kappa of 0.87). This result indicates that to discriminate between TP and TRC, looking for signs of radionecrosis (blood-brain barrier disruption areas, as assessed with T1G sequence, without sufficiently matched intense F-DOPA uptake) may be as useful as looking for signs of viable tumor. The SWI/PET accuracy was also good (81%) but the interobserver agreement was slightly lower (Kappa of 0.66). This result indicates that carefully considering regions where hemorrhagic changes occurred, as depicted by SWI MRI sequences, is useful when interpreting F-DOPA PET. By design, SWI/PET was less sensitive to diagnose TP than conventional analysis (79% vs. 92%) but it proved to be much more specific (83% vs. 57%). It should be noted that these results may not apply to FET. Indeed, macrophagic uptake of FET has been shown to be weaker than that of other amino acid radiotracers in animal models of brain injury [23]. As brain bleeding can be responsible for macrophagic infiltration [24], FET-PET may be less sensitive to these phenomena. Lastly, the presence of F-DOPA PET uptakes away from contrast-

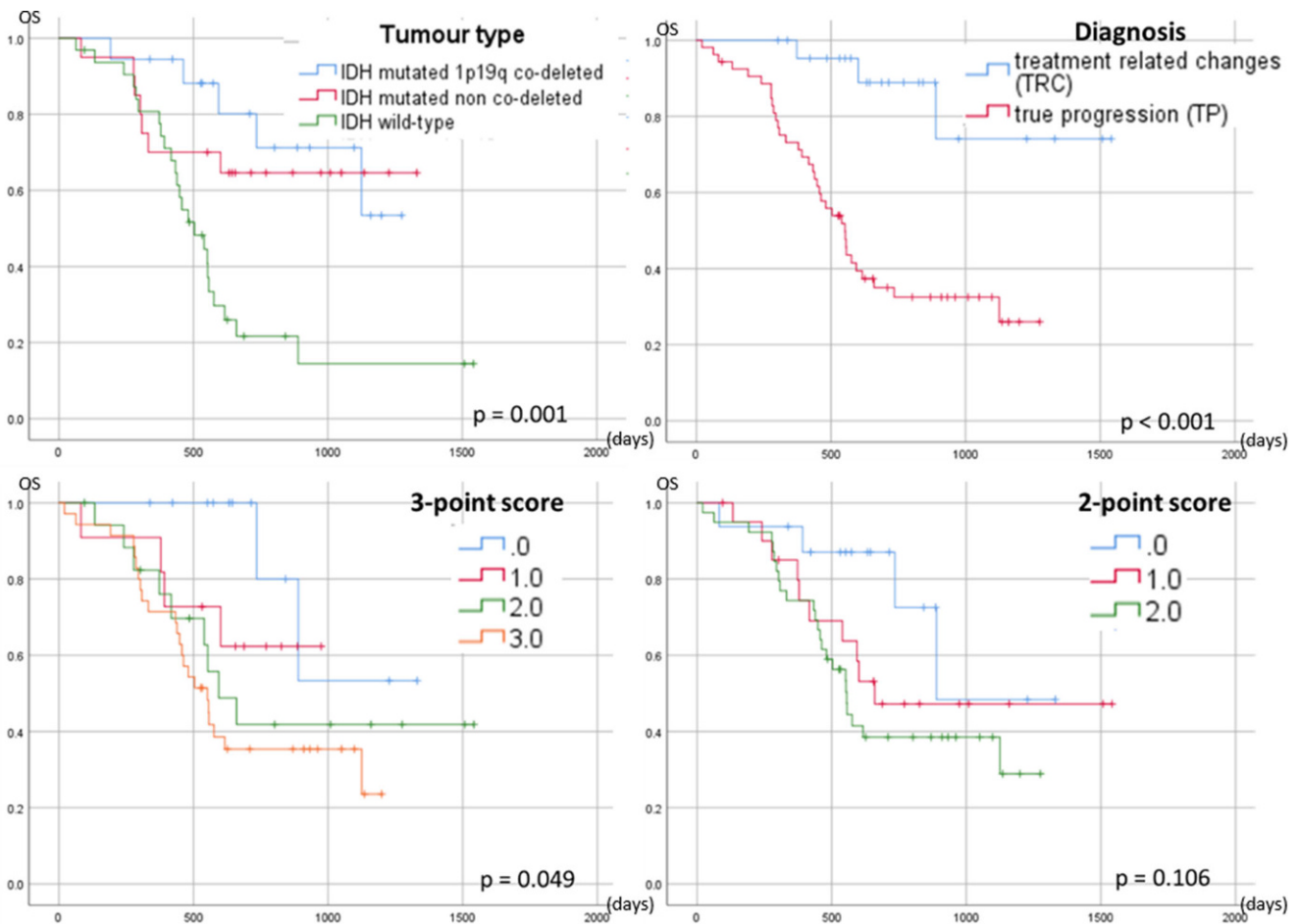


Fig. 3 Kaplan-Meier survival curves. Overall survival curves according to tumor type, final diagnosis for lesions evolution at the time of F-DOPA PET/MRI, 3-point score, and 2-point score. Both tumor type, final diagnosis and 3-point score are significantly associated with overall survival

enhanced areas (TIG-/PET (+)) and in the white matter (WM/PET (+)), which were supposed to depict respectively non-enhanced glioma infiltration and glioma tissue in the white matter, was of limited value to discriminate between TP and TRC in our patients.

The ASL rCBF ratio showed good performances in our study. With the best cut-off at 1.25, it was able to discriminate between TP and TRC with an accuracy of 84%. We chose to study pseudocontinuous ASL because it is known to be less sensitive to magnetic susceptibility artefacts than gradient-echo based DSC [25]. The literature on the value of ASL perfusion in this setting is still scarce but it is known to correlate well with DSC [26]. In a study carried out on 32 patients treated by chemoradiotherapy for a glioblastoma, pseudo-continuous ASL performed particularly well to discriminate pseudoprogression from TP, with an AUC of 0.95 for a cut-off at 1.57 [27]. In another study on 33 patients treated with proton beam therapy for high-grade glioma, ASL had better sensitivity (94%) than DSC, using an rCBF ratio cut-off value of 1.3 [28]. Finally, our team has recently shown the good performances

of an automatic and parametric analysis of ASL sequences and F-DOPA PET in the differential diagnosis between progression and pseudoprogression. In this previous study, the combined performance of the two techniques was excellent (sensitivity 94% and specificity 100%) but this required complex preprocessing of the images and could only be applied to lesions involving only one of the two cerebral hemispheres [29]. On the other hand, our use of ASL sequence in the present work was unusual because both morphologic MRI sequences and F-DOPA-PET images were used to guide ROIs positioning. PET allowed positioning ROIs in small metabolic tumor “hot spots” with rCBF ≥ 1.25 despite the absence of a visually obvious hyperperfused area in some patients. In others with lesions involving the cortex or near vessels, it helped to discriminate physiological features from tumor-related hyperperfusion. We think ASL sequences are particularly well suited for F-DOPA PET/MRI in neuro-oncology as they are less sensitive to hemorrhagic changes than DSC and may help mitigate the lower specificity of F-DOPA PET in hemorrhagic lesions. DSC sequences were also acquired in our patients but were

Table 5 Overall survival analyses

Univariate analyses				
Variable		<i>p</i> -value	HR	95% IC
Tumor type	<i>IDH</i> _{WT}	0.001	Not applicable (reference)	Not applicable
	<i>IDH</i> _{m-non-codel}	0.004	0.3	0.1–0.7
	<i>IDH</i> _{m-codel}	0.004	0.2	0.1–0.6
T1G+/PET (+)		0.15	1.8	0.8–3.9
T1G-/PET (+)		0.55	1.2	0.6–2.3
WM/PET (+)		0.01	2.6	1.3–5.4
SWI/PET (+)		0.04	2.1	1.0–4.4
TBR ≥ 3.7		0.02	2.4	1.2–4.7
<i>rCBF</i> ratio ≥ 1.25		0.001	4.1	1.6–10.5
<i>rCBF</i> ratio ≥ 2.7		<0.001	4.1	2.1–8.0
Enhancement size ≥ 135 mm ²		0.02	2.7	1.1–6.4
3-point score		0.007	1.6 ^a	1.1–2.3 ^a
2-point score		0.039	1.6 ^a	1.0–2.5 ^a
Diagnosis = TP		<0.001	6.9	2.1–22.6
Multivariate analysis				
Variable		<i>p</i> -value	HR	95% IC
Tumor type	<i>IDH</i> _{WT}	0.02	Not applicable (reference)	Not applicable
	<i>IDH</i> _{m-non-codel}	0.03	0.4	0.2–0.9
	<i>IDH</i> _{m-codel}	0.02	0.3	0.1–0.8
WM/PET (+)		0.14	1.8	0.8–4.0
<i>rCBF</i> ratio ≥ 2.7		0.03	2.3	1.1–4.8
Enhancement size ≥ 135 mm ²		0.50	1.4	0.5–3.6

Most PET, MRI and hybrid parameters are predictors of OS in univariate analysis. The type of tumor as assessed by the molecular profile is also a strong prognostic factor. Compared to *IDH*_{WT} gliomas, taken as a reference, prognostic was better in *IDH*_{m-non-codel} and *IDH*_{m-codel} gliomas. In multivariate analysis, only tumor type and *rCBF* ≥ 2.7 appear as independent prognostic factors

HR hazard ratio for overall survival (OS), 95% IC confidence interval for HR, TP true progression, as assessed retrospectively, *rCBF* regional cerebral blood flow

^aHR for 1-unit increase

deemed to be at risk of false negative results due to hemorrhagic changes in several of them. The direct comparison between ASL and DSC was beyond the scope of this article and could be biased in our study. With this reservation, the accuracy of regional cerebral blood volume ratios as calculated with DSC was lower, although not significantly, than that of ASL *rCBF*, with an AUC of 0.77 and an accuracy of 71% for the best cut-off value of 1.59.

Having selected among our imaging parameters through logistic regression analyses, we created a 3-point score, based on two morphometabolic parameters and ASL *rCBF*. It classified patients more accurately than any individual parameter, with an AUC of 0.93 and an accuracy of 87%. The performance of our 3-point score is similar to that found for the sequential use of DSC and FET-PET in a study by Steidl et al. on 104 patients with accuracies of 87% and 83% (with leave one out cross-validation), respectively [30]; however, our score offers a more balanced distribution between sensitivity and specificity than their algorithm, with sensitivities of 91% versus 96%, and specificities of 78% vs. 25%, respectively. We also created a 2-point score that only included T1G-/PET and SWI/PET, to be used when ASL

perfusion is not available, whose performances appeared slightly but not significantly lower than the 3-point score. Indeed, extreme values of both scores were very reliable for establishing or excluding TP. Nevertheless, a 2-point score of 1 was associated with major diagnostic uncertainty and should probably be followed by further investigations.

In our study, *IDH*_{m-non-codel} gliomas exhibited significantly lower uptake than other tumor types, as previously described with F-DOPA [31] and FET [32]. We found no significant impact of tumor molecular type on the accuracy of PET parameters in our patients as it has been shown with FET [33] but this study is probably underpowered to demonstrate such an effect. Nevertheless, the best diagnostic accuracy using standard interpretation criteria or our own was obtained in *IDH*_{m-codel} gliomas (94%), which had the highest FDOPA uptake. Lastly, our OS analyses confirmed that a diagnosis of TRC was indeed associated with a better prognosis than a diagnosis of TP. In univariate analysis, most PET, MRI, and hybrid parameters were associated with OS, as well as both 2 and 3-point scores. Interestingly, we found that T1G+/PET was not predictive of OS despite its usefulness to differentiate between TP and TRC.

This result makes sense as TIG+/PET was meant to look for signs of radionecrosis and not viable tumor tissue and when only the latter is supposed to impact OS. Nevertheless, no F-DOPA-PET parameter was found to be independently associated with OS in multivariate analysis, whereas glioma molecular profile and ASL rCBF were. The fact that IDH_{m-codel} gliomas are usually associated with intense PET uptake and a good prognosis probably contributes to the lower F-DOPA-PET predictive value regarding OS [34, 35]; however, multivariate analyses results were not significantly modified after patients with IDH_{m-codel} tumors were excluded. Our result thus falls between that of Karunanithi et al. [36], who found a strong prognostic value for F-DOPA PET in a cohort of 33 patients with a suspicion of glioma recurrence, and that of Herrmann et al. [8], who found no prognostic value of OS for any of the F-DOPA parameters they studied. It is also consistent with those of Fueger et al. who found a correlation between F-DOPA uptake and tumor grade as well as Ki-67 proliferation index in treatment-naïve glioma but not in recurrent tumors [37].

Our study has several limitations. Firstly, we used histological diagnosis as the gold standard for only 20% of our patients, as in many previous investigations. A discussion about the relative value of histological analysis and retrospective diagnosis based on glioma recurrence follow-up is beyond the scope of this article. Nevertheless, our patients were included consecutively, and are probably quite representative of the population seen in amino acid PET in the clinical routine setting. Secondly, we analyzed patients irrespective of the postradiotherapy delay, mixing pseudo-progression and radionecrosis diagnoses. As we found no significant differences in the parameters' performance between the patients seen within 6 months of their last radiation therapy or chemotherapy and the others, we believe that our results apply in both settings. Because of the limited sample size, we were not able to study the impact of MGMT promoter methylation status of tumors, known to be linked with an increased risk of pseudoprogression [38]. Thirdly, our PET and MRI analyses were blinded to previous MRI and examination request. This is not insignificant as the area where MRI abnormalities worsened or appeared is supposed to be specifically analyzed in PET. In this respect, our results do not fully reflect best clinical practice; however, the co-existence of TRC and viable tumor tissue is frequently found in patients treated for glioma. Our parameters and scores, which consider the whole brain, allow reaching a simple conclusion in all cases, with good accuracy, and without analysis of previous MRI. Moreover, many patients referred for amino acid PET during the follow-up of their glioma are undergoing systemic treatment. For them, it should be kept in mind that even if the question asked by the clinician is usually to differentiate TP from TRC for specific MRI modifications, what has to be decided

is whether to continue or change the systemic treatment. Thus, PET uptakes can be of clinical importance regardless of their localization in the brain. Yet, we acknowledge that in the absence of baseline F-DOPA PET, differentiating an uptake due to residual tumor tissue that is well controlled by treatment from TP can be impossible. Lastly, we used logistic regression results to generate our hybrid scores, using the relative weights of statistically significant predictive factors. In this respect, correlations between studied parameters and multicollinearity could have influenced our results and this is why we verified that they were low enough. These logistic regressions were performed with bootstrap analysis to reduce the risk of overfitting. With scores involving only 2 or 3 parameters of equal weight, we consider this risk as reasonably low.

In conclusion, we propose practical hybrid F-DOPA-PET and MRI interpretation criteria and scores to be used in patients with a suspicion of glioma recurrence. Our 3-point score performed better than the F-DOPA PET conventional method of interpretation in this exploratory study. These results should be confirmed prospectively. How it compares exactly with the sequential use of different MRI perfusion methods and PET quantitative analysis would also be interesting to study but requires a large number of patients.

Supplementary Information The online version of this article (<https://doi.org/10.1007/s00062-022-01139-0>) contains supplementary material, which is available to authorized users.

Funding No funding was received for conducting this study.

Author Contribution All the authors contributed to the study conception and design. Material preparation, data collection, and analysis were performed by Marc Bertaux, Caroline Dehais, Laura Rozenblum, Laure-Eugenie Tainturier, and Aurelie Kas. Blind examination of images was performed by Arnaud Berenbaum and Marc Bertaux. The first draft of the manuscript was written by Marc Bertaux and all the authors have commented on the previous versions of the manuscript. All the authors read and approved the final manuscript.

Conflict of interest M. Bertaux, A. Berenbaum, A.-L. Di Stefano, L. Rozenblum, M. Soret, S. Bergeret, K. Hoang-Xuan, L.-E. Tainturier, B. Sgard, M.-O. Habert, J.-Y. Delattre, C. Dehais, A. Idhah, N. Pyatigorskaya and A. Kas declare that they have no competing interests.

References

1. Patel P, Baradaran H, Delgado D, Askin G, Christos P, John Tsiouris A, Gupta A. MR perfusion-weighted imaging in the evaluation of high-grade gliomas after treatment: a systematic review and meta-analysis. *Neuro Oncol.* 2017;19:118-27.
2. Xu Q, Liu Q, Ge H, Ge X, Wu J, Qu J, Xu K. Tumor recurrence versus treatment effects in glioma: A comparative study of three dimensional pseudo-continuous arterial spin labeling and dynamic susceptibility contrast imaging. *Medicine (Baltimore).* 2017;96:e9332.
3. Albert NL, Weller M, Suchorska B, Galldiks N, Soffietti R, Kim MM, la Fougère C, Pope W, Law I, Arbuzo J, Chamberlain MC,

- Vogelbaum M, Ellingson BM, Tonn JC. Response Assessment in Neuro-Oncology working group and European Association for Neuro-Oncology recommendations for the clinical use of PET imaging in gliomas. *Neuro Oncol.* 2016;18:1199-208.
4. Chen W, Silverman DH, Delaloye S, Czernin J, Kamdar N, Pope W, Satyamurthy N, Schiepers C, Cloughesy T. 18F-FDOPA PET imaging of brain tumors: comparison study with 18F-FDG PET and evaluation of diagnostic accuracy. *J Nucl Med.* 2006;47:904-11.
 5. Treglia G, Muoio B, Trevisi G, Mattoli MV, Albano D, Bertagna F, Giovanella L. Diagnostic Performance and Prognostic Value of PET/CT with Different Tracers for Brain Tumors: A Systematic Review of Published Meta-Analyses. *Int J Mol Sci.* 2019;20:4669.
 6. Yu J, Zheng J, Xu W, Weng J, Gao L, Tao L, Liang F, Zhang J. Accuracy of 18F-FDOPA Positron Emission Tomography and 18F-FET Positron Emission Tomography for Differentiating Radiation Necrosis from Brain Tumor Recurrence. *World Neurosurg.* 2018;114:e1211-24.
 7. Xiao J, Jin Y, Nie J, Chen F, Ma X. Diagnostic and grading accuracy of 18F-FDOPA PET and PET/CT in patients with gliomas: a systematic review and meta-analysis. *BMC Cancer.* 2019;19:767.
 8. Herrmann K, Czernin J, Cloughesy T, Lai A, Pomykala KL, Benz MR, Buck AK, Phelps ME, Chen W. Comparison of visual and semiquantitative analysis of 18F-FDOPA-PET/CT for recurrence detection in glioblastoma patients. *Neuro Oncol.* 2014;16:603-9.
 9. Galldiks N, Stoffels G, Filss C, Rapp M, Blau T, Tscherpel C, Ceccon G, Dunkl V, Weinzierl M, Stoffel M, Sabel M, Fink GR, Shah NJ, Langen KJ. The use of dynamic O-(2-18F-fluoroethyl)-L-tyrosine PET in the diagnosis of patients with progressive and recurrent glioma. *Neuro Oncol.* 2015;17:1293-300.
 10. Kebir S, Fimmers R, Galldiks N, Schäfer N, Mack F, Schaub C, Stuplich M, Niessen M, Tzaridis T, Simon M, Stoffels G, Langen KJ, Scheffler B, Glas M, Herrlinger U. Late Pseudoprogession in Glioblastoma: Diagnostic Value of Dynamic O-(2-[18F]fluoroethyl)-L-Tyrosine PET. *Clin Cancer Res.* 2016;22:2190-6.
 11. Zaragori T, Ginet M, Marie PY, Roch V, Grignon R, Gauchotte G, Rech F, Blonski M, Lamiral Z, Taillandier L, Imbert L, Verger A. Use of static and dynamic [18F]-F-DOPA PET parameters for detecting patients with glioma recurrence or progression. *EJNMMI Res.* 2020;10:56.
 12. Law I, Albert NL, Arbizu J, Boellaard R, Drzezga A, Galldiks N, la Fougère C, Langen KJ, Lopci E, Lowe V, McConathy J, Quick HH, Sattler B, Schuster DM, Tonn JC, Weller M. Joint EANM/EANO/RANO practice guidelines/SNMMI procedure standards for imaging of gliomas using PET with radiolabelled amino acids and [18F]FDG: version 1.0. *Eur J Nucl Med Mol Imaging.* 2019;46:540-57.
 13. Pyka T, Hiob D, Preibisch C, Gempt J, Wiestler B, Schlegel J, Straube C, Zimmer C. Diagnosis of glioma recurrence using multiparametric dynamic 18F-fluoroethyl-tyrosine PET-MRI. *Eur J Radiol.* 2018;103:32-7.
 14. Fraioli F, Shankar A, Hyare H, Ferrazzoli V, Militano V, Samandouras G, Mankad K, Solda F, Zaccagna F, Mehdi E, Lyasheva M, Bomanji J, Novruzov F. The use of multiparametric 18F-fluoro-L-3,4-dihydroxy-phenylalanine PET/MRI in post-therapy assessment of patients with gliomas. *Nucl Med Commun.* 2020;41:517-25.
 15. Sala Q, Metellus P, Taieb D, Kaphan E, Figarella-Branger D, Guedj E. 18F-DOPA, a clinically available PET tracer to study brain inflammation? *Clin Nucl Med.* 2014;39:e283-5.
 16. Dethy S, Manto M, Kentos A, Konopnicki D, Pirotte B, Goldman S, Hildebrand J. PET findings in a brain abscess associated with a silent atrial septal defect. *Clin Neurol Neurosurg.* 1995;97:349-53.
 17. Morana G, Bottoni G, Mancardi MM, Verrico A, Piccardo A. Seizure-Induced Increased 18F-DOPA Uptake in a Child With Diffuse Astrocytoma and Transient Brain MRI Abnormalities Related to Status Epilepticus. *Clin Nucl Med.* 2018;43:e149-50.
 18. Ogawa T, Hatazawa J, Inugami A, Murakami M, Fujita H, Shimosegawa E, Noguchi K, Okudera T, Kanno I, Uemura K, et al. Carbon-11-methionine PET evaluation of intracerebral hematoma: distinguishing neoplastic from non-neoplastic hematoma. *J Nucl Med.* 1995;36:2175-9.
 19. Wen PY, Macdonald DR, Reardon DA, Cloughesy TF, Sorensen AG, Galanis E, Degroot J, Wick W, Gilbert MR, Lassman AB, Tsien C, Mikkelsen T, Wong ET, Chamberlain MC, Stupp R, Lamborn KR, Vogelbaum MA, van den Bent MJ, Chang SM. Updated response assessment criteria for high-grade gliomas: response assessment in neuro-oncology working group. *J Clin Oncol.* 2010;28:1963-72.
 20. Weller M, van den Bent M, Tonn JC, Stupp R, Preusser M, Cohen-Jonathan-Moyal E, Henriksson R, Le Rhun E, Balana C, Chinot O, Bendszus M, Reijneveld JC, Dhermain F, French P, Marosi C, Watts C, Oberg I, Pilkington G, Baumert BG, Taphoorn MJB, Hegi M, Westphal M, Reifenberger G, Soffietti R, Wick W; European Association for Neuro-Oncology (EANO) Task Force on Gliomas. European Association for Neuro-Oncology (EANO) guideline on the diagnosis and treatment of adult astrocytic and oligodendroglial gliomas. *Lancet Oncol.* 2017;18:e315-29. Erratum in: *Lancet Oncol.* 2017;18:e642.
 21. Wollenweber SD, Ambwani S, Delso G, Lonn AHR, Mullick R, Wiesinger F, Piti Z, Tari A, Novak G, Fidrich M. Evaluation of an Atlas-based PET head attenuation correction using PET/CT & MR patient data. *IEEE Trans Nucl Sci.* 2013;60:3383-90.
 22. Youden WJ. Index for rating diagnostic tests. National bureau of standards; Washington D.C.: 1949.
 23. Salber D, Stoffels G, Pauleit D, Oros-Peusquens AM, Shah NJ, Klauth P, Hamacher K, Coenen HH, Langen KJ. Differential uptake of O-(2-18F-fluoroethyl)-L-tyrosine, L-3H-methionine, and 3H-deoxyglucose in brain abscesses. *J Nucl Med.* 2007;48:2056-62.
 24. Tschoe C, Bushnell CD, Duncan PW, Alexander-Miller MA, Wolfe SQ. Neuroinflammation after Intracerebral Hemorrhage and Potential Therapeutic Targets. *J Stroke.* 2020;22:29-46.
 25. Choi YJ, Kim HS, Jahng GH, Kim SJ, Suh DC. Pseudoprogession in patients with glioblastoma: added value of arterial spin labeling to dynamic susceptibility contrast perfusion MR imaging. *Acta Radiol.* 2013;54:448-54.
 26. Jovanovic M, Radenkovic S, Stosic-Opincal T, Lavrnica S, Gavrilovic S, Lazovic-Popovic B, Soldatovic I, Maksimovic R. Differentiation between progression and pseudoprogession by arterial spin labeling MRI in patients with glioblastoma multiforme. *J BUON.* 2017;22:1061-7.
 27. Manning P, Daghighi S, Rajaratnam MK, Parthiban S, Bahrami N, Dale AM, Bolar D, Piccioni DE, McDonald CR, Farid N. Differentiation of progressive disease from pseudoprogession using 3D PCASL and DSC perfusion MRI in patients with glioblastoma. *J Neurooncol.* 2020;147:681-90.
 28. Ozsunar Y, Mullins ME, Kwong K, Hochberg FH, Ament C, Schaefer PW, Gonzalez RG, Lev MH. Glioma recurrence versus radiation necrosis? A pilot comparison of arterial spin-labeled, dynamic susceptibility contrast enhanced MRI, and FDG-PET imaging. *Acad Radiol.* 2010;17:282-90.
 29. Pellerin A, Khalifé M, Sanson M, Rozenblum-Beddok L, Bertaux M, Soret M, Galanaud D, Dormont D, Kas A, Pyatigorskaya N. Simultaneously acquired PET and ASL imaging biomarkers may be helpful in differentiating progression from pseudo-progression in treated gliomas. *Eur Radiol.* 2021;31:7395-405.
 30. Steidl E, Langen KJ, Hmeidani SA, Polomac N, Filss CP, Galldiks N, Lohmann P, Keil F, Filipinski K, Mottaghy FM, Shah NJ, Steinbach JP, Hattingen E, Maurer GD. Sequential implementation of DSC-MR perfusion and dynamic [18F]FET PET allows efficient differentiation of glioma progression from treatment-related changes. *Eur J Nucl Med Mol Imaging.* 2021;48:1956-65.

31. Tatekawa H, Hagiwara A, Yao J, Oughourlian TC, Ueda I, Uetani H, Raymond C, Lai A, Cloughesy TF, Nghiemphu PL, Liao LM, Pope WB, Salamon N, Ellingson BM. Voxelwise and Patientwise Correlation of 18F-FDOPA PET, Relative Cerebral Blood Volume, and Apparent Diffusion Coefficient in Treatment-Naïve Diffuse Gliomas with Different Molecular Subtypes. *J Nucl Med.* 2021;62:319-25.
32. Suchorska B, Giese A, Biczok A, Unterrainer M, Weller M, Drexler M, Bartenstein P, Schüller U, Tonn JC, Albert NL. Identification of time-to-peak on dynamic 18F-FET-PET as a prognostic marker specifically in IDH1/2 mutant diffuse astrocytoma. *Neuro Oncol.* 2018;20:279-88.
33. Maurer GD, Brucker DP, Stoffels G, Filipski K, Filss CP, Mottaghy FM, Galldiks N, Steinbach JP, Hattingen E, Langen KJ. 18F-FET PET Imaging in Differentiating Glioma Progression from Treatment-Related Changes: A Single-Center Experience. *J Nucl Med.* 2020;61:505-11.
34. Jansen NL, Schwartz C, Graute V, Eigenbrod S, Lutz J, Egensperger R, Pöpperl G, Kretzschmar HA, Cumming P, Bartenstein P, Tonn JC, Kreth FW, la Fougère C, Thon N. Prediction of oligodendroglial histology and LOH 1p/19q using dynamic [(18)F]FET-PET imaging in intracranial WHO grade II and III gliomas. *Neuro Oncol.* 2012;14:1473-80.
35. Tabouret E, Nguyen AT, Dehais C, Carpentier C, Ducray F, Id-baih A, Mokhtari K, Jouvet A, Uro-Coste E, Colin C, Chinot O, Loiseau H, Moyal E, Maurage CA, Polivka M, Lechapt-Zalcman E, Desenclos C, Meyronet D, Delattre JY, Figarella-Branger D; For POLA Network. Prognostic impact of the 2016 WHO classification of diffuse gliomas in the French POLA cohort. *Acta Neuropathol.* 2016;132:625-34.
36. Karunanithi S, Sharma P, Kumar A, Gupta DK, Khangembam BC, Ballal S, Kumar R, Kumar R, Bal C. Can (18)F-FDOPA PET/CT predict survival in patients with suspected recurrent glioma? A prospective study. *Eur J Radiol.* 2014;83:219-25.
37. Fueger BJ, Czernin J, Cloughesy T, Silverman DH, Geist CL, Walter MA, Schiepers C, Nghiemphu P, Lai A, Phelps ME, Chen W. Correlation of 6-18F-fluoro-L-dopa PET uptake with proliferation and tumor grade in newly diagnosed and recurrent gliomas. *J Nucl Med.* 2010;51:1532-8.
38. Brandes AA, Franceschi E, Tosoni A, Blatt V, Pession A, Tallini G, Bertorelle R, Bartolini S, Calbucci F, Andreoli A, Frezza G, Leonardi M, Spagnoli F, Ermani M. MGMT promoter methylation status can predict the incidence and outcome of pseudoprogression after concomitant radiochemotherapy in newly diagnosed glioblastoma patients. *J Clin Oncol.* 2008;26:2192-7.